NANO LETTERS

Letter

pubs.acs.org/NanoLett

A Selection for Assembly Reveals That a Single Amino Acid Mutant of the Bacteriophage MS2 Coat Protein Forms a Smaller Virus-like Particle

Michael A. Asensio,[†] Norma M. Morella,[‡] Christopher M. Jakobson,[§] Emily C. Hartman,[∥] Jeff E. Glasgow,[∥] Banumathi Sankaran,[⊥,#] Peter H. Zwart,[⊥,#] and Danielle Tullman-Ercek*[,#,%]

[†]Department of Bioengineering, [‡]Department of Plant and Microbial Biology, [§]Department of Chemical and Biomolecular Engineering, and [∥]Department of Chemistry, University of California, Berkeley, Berkeley, California 94720, United States

[⊥]Berkeley Center for Structural Biology and [#]Molecular Biophysics and Integrated Bioimaging, Lawrence Berkeley National Laboratory, Berkeley, California 94720, United States

[%]Department of Chemical and Biological Engineering, Northwestern University, Evanston, Illinois 60091, United States

Supporting Information

ABSTRACT: Virus-like particles are used to encapsulate drugs, imaging agents, enzymes, and other biologically active molecules in order to enhance their function. However, the size of most virus-like particles is inflexible, precluding the design of appropriately sized containers for different applications. Here, we describe a chromatographic selection for virus-like particle assembly. Using this selection, we identified a single amino acid substitution to the coat protein of bacteriophage MS2 that mediates a uniform switch in particle geometry from $T = 3$ to $T = 1$ icosahedral symmetry. The resulting smaller particle retains the ability to be disassembled and reassembled *in vitro* and to be chemically modified to load cargo into its interior cavity. The pair of 27 and 17 nm MS2 particles will allow direct examination of the effect of size on function in established applications of virus-like particles, including drug delivery and imaging.

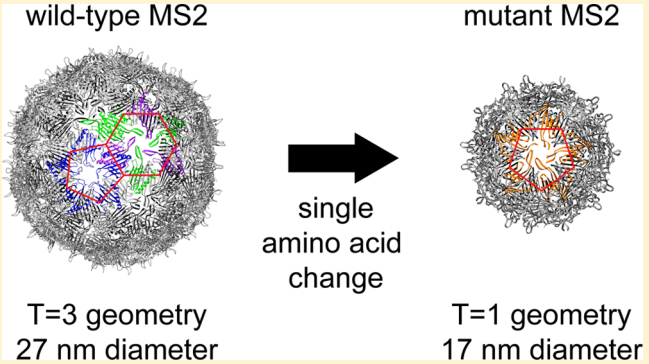

KEYWORDS: *Protein engineering, protein supramolecular structure, virus structure, bacteriophage MS2, drug delivery, nanocontainers*

Virus-like particles are attractive scaffolds for nanoengineering. These particles are chemically and thermally stable, easy to produce and assemble, and can be genetically modified to encode changes to the protein nanostructure. Viral capsids and virus-like particles have found applications as drug delivery vehicles,[1] imaging agents,[2,3] nanobioreactors,[4−6] light harvesting arrays,[7] and templates for inorganic synthesis.[8,9] Many strategies have been developed to decorate the interior and exterior of such structures with useful chemical moieties[10−12] and to encapsulate functional cargo in the cavity of these structures.[13−16] To date, a key limitation of virus-like particles as drug delivery and imaging agents is the inability to tune particle size to optimize serum half-life and tissue penetrance.[17] We therefore set out to find variants of the MS2 bacteriophage coat protein that formed smaller virus-like particles, enabling the comparison of protein containers of different size but nearly identical chemical composition.

MS2 bacteriophage virus-like particles have been investigated for nanoscale patterning, drug delivery, and the study of enzyme encapsulation. Each wild-type MS2 particle forms an icosahedral capsid of approximately 27 nm in diameter. Natively, each capsid consists of 178 copies of the coat protein (CP) and one copy of the maturation protein (Mat, or A-protein).[18,19] Importantly, MS2 coat protein can be recombinantly expressed and assembled *in vitro* to form an icosahedral virus-like particle (VLP).[14] These VLPs are of particular interest in nanoengineering, in part due to their amenability to chemical modifications and ability to disassemble and reassemble *in vitro* around diverse forms of cargo.[10−12,14] The CP can also tolerate several amino acid mutations that render it more amenable to targeted post-translational modifications for various applications.[12,20−22]

In phage and VLPs, the MS2 CP forms dimers that assemble into an icosahedron with 12 pentameric and 20 hexameric faces—a so-called $T = 3$ geometry. The structure of MS2 particles has been extensively characterized,[23−26,14] but, as with other multimeric assemblies, no point mutations are known to confer uniform changes in the icosahedral supramolecular structure adopted by the CP. If these could be identified, the

Received: July 15, 2016
Revised: August 16, 2016
Published: August 23, 2016

DOI: 10.1021/acs.nanolett.6b02948
Nano Lett. 2016, 16, 5944−5950

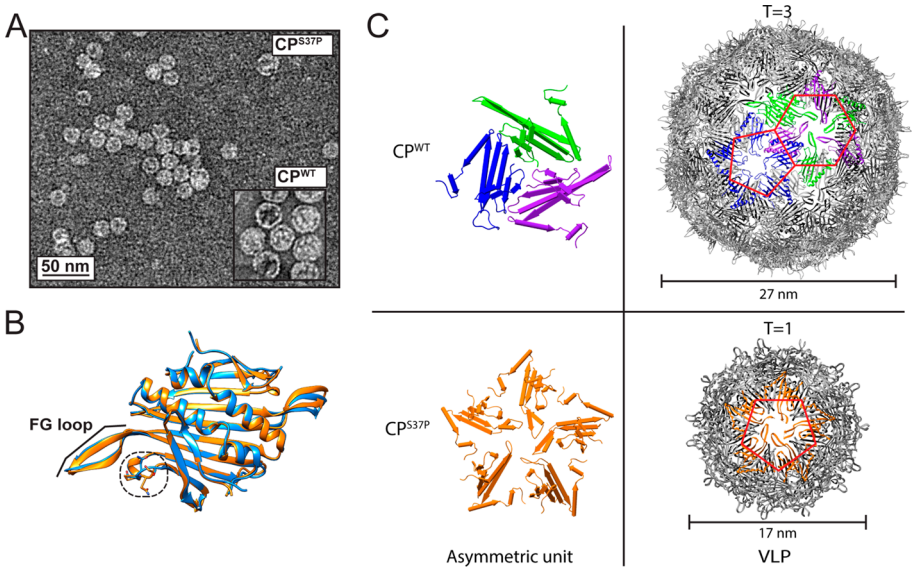

Figure 1. CP^{S37P} dimers form a VLP of 17 nm diameter with a $T = 1$ icosahedral structure. (A) Transmission electron micrograph of CP^{S37P} VLPs and CP^{WT} VLPs (inset). (B) Structural alignment of CP^{S37P} (orange) and CP^{WT} (blue) dimer structures. (C) Crystallographic asymmetric unit structures (left) and complete VLP structures (right) from crystal structures of CP^{WT} (top; 2MS2) and CP^{S37P} (bottom; 4ZOR) VLPs. Hexameric and pentameric capsomeres are outlined in red to highlight the $T = 1$ and $T = 3$ icosahedral geometries.

mutants would serve as useful tools for exploring the effects of VLP size on engineered MS2 VLP performance for drug delivery and imaging applications. Additionally, these unique structural variants may also shed light on the structural evolutionary landscape of the common $T = 3$ viral geometry.

Here we report that a single amino acid change to the MS2 CP confers a radical change in the MS2 VLP supramolecular structure from a $T = 3$ icosahedron of 27 nm diameter to a $T = 1$ icosahedron of approximately 17 nm diameter consisting of 12 pentamers. This MS2 CP variant retains a similar dimer conformation to the wild type, despite adopting a smaller capsid structure. Moreover, it remains amenable to *in vitro* reassembly, supports the incorporation of the Mat protein that is required for infection, and tolerates a mutation that was previously used to perform *in vitro* coupling of small molecules to the interior of the MS2 VLP. Many applications of MS2 VLPs will therefore extend to this new structure, allowing a side-by-side comparison of chemically similar VLPs of different sizes. These results also provide new insights into long-standing debates on the evolution of viruses and gene-transfer agents as well as the possibility for multiple stable forms of multiprotein assemblies. Finally, we expect this work to inspire new possibilities for the computational design of made-to-order protein-based nanomaterials.

In order to identify mutants of the MS2 *cp* gene that encode CP variants retaining the ability to assemble into VLPs, error-prone PCR was used to generate a pool of mutated MS2 *cp* genes (for details of this and other experimental procedures, see the Methods section in the Supporting Information). Approximately five nucleotide mutations were introduced in each gene relative to the wild type, and the final library size was approximately 10^5 unique *cp* genes. The mutant genes were expressed in *E. coli* (one copy per bacterial cell), and the resulting naïve pool was subjected to a chromatographic selection for VLP assembly. The selection used was the same procedure typically used to purify CP^{WT} VLPs from *E. coli*. Since each assembly competent VLP encapsulated the nucleic acids encoding the peptides in its shell, deep sequencing of the nucleic acids (DNA and RNA) from the naïve library and selected pool was used to reveal *cp* genes enriched by selection for assembly. We focused on mutants identified after one round of VLP packaging, that is, plasmid-based expression in *E. coli* and purification by precipitation followed by ion exchange and size exclusion chromatography to isolate VLP-sized particles. These VLPs were subjected to disruption and nucleic acid isolation, followed by sequencing.[27] We assessed enrichment at each amino acid position by comparing the Shannon information theoretic entropy at each position and discovered that only residue Ser37 demonstrated an increase in Shannon entropy upon selection (Supporting Information Figure S1). Upon closer inspection, we were surprised to find that 70.5% of the reads in the pool selected for assembly encoded a Ser37Pro mutation (as compared to 2.8% of reads in the naïve library). This mutation is observed in the literature only twice, arising from selections in two separate directed evolution studies by Peabody and colleagues, but it was not pursued further in either study and was not characterized for size.[28,29] Given that the mutation arose only when selections did not include an infection step, we speculated that perhaps this variation does not yield infectious particles, precluding its observation in the myriad other evolutionary studies of MS2 VLPs. We therefore sought to examine the structural and biochemical properties of this highly abundant CP^{S37P} variant. The abundance of other amino acid mutations in the selected pool is shown relative to the naïve library at each residue of the CP protein in Figure S2.

The mutant *cp* gene encoding the CP^{S37P} mutant was recapitulated and expressed in *E. coli*, and the resulting VLPs exhibited similar properties to wild-type MS2 capsids throughout purification. Remarkably, transmission electron microscopy (TEM) revealed that the particles formed of CP^{S37P} are smaller than the VLPs formed by the wild-type CP (Figure 1A). This observation was confirmed by dynamic light scattering and size-exclusion chromatography (Figure S3). We hypothesized that this smaller particle was likewise formed from CP dimers but assembled into a different geometry. We therefore crystallized the CP^{S37P} VLP and determined its

DOI: 10.1021/acs.nanolett.6b02948
Nano Lett. 2016, 16, 5944−5950

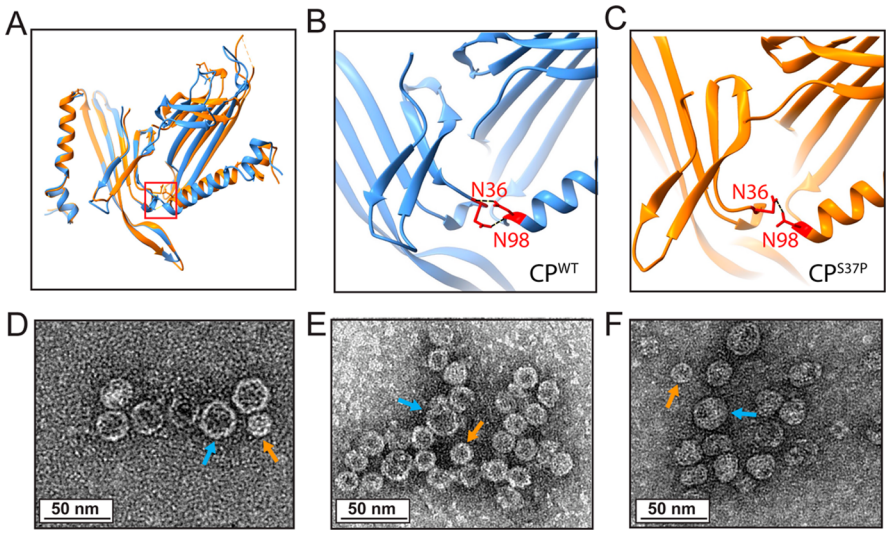

Figure 2. Hydrogen bonding contributes to the stability of $T = 1$ icosahedral CP^{S37P} VLPs. (A) Structural alignment of CP^{S37P} (orange) and CP^{WT} (blue) interdimer interface structures. Residues in (B) CP^{WT} and (C) CP^{S37P} structure altered to probe hydrogen-bonding interactions. Transmission electron micrographs of VLPs formed of (D) $CP^{N36A/S37P}$, (E) $CP^{S37P/N98A}$, and (F) $CP^{N36A/S37P/N98A}$. Blue arrows indicate VLPs of CP^{WT} size (27 nm); orange arrows indicate VLPs of CP^{S37P} size (17 nm).

structure by X-ray diffraction. The structures of the pentameric asymmetric unit (ASU) and $T = 1$ icosahedral VLP of CP^{S37P} (PDB ID: 4ZOR) are shown alongside the structures of the trimeric ASU and $T = 3$ icosahedral VLP of CP^{WT} (PDB ID: 2MS2) (Figure 1C). Crystallographic statistics can be found in Table S1, and a stereoscopic projection of a portion of electron density map can be found in Figure S4. The five peptide chains in the CP^{S37P} ASU have nearly identical conformations but differ slightly in the "FG" loop, which surrounds the pore in the center of the pentamer and lies in a region known to affect assembly.[25,26] Interestingly, the proline residue at position 37 adopts a *cis* conformation in all five chains of the CP^{S37P} ASU, in contrast to the *trans* serine residue present at this position in the CP^{WT} VLP. This results in a slight but clear difference in the conformation of a small loop directly adjacent to the S37P mutation (Figure 1B). Notably, the interior volume of the CP^{S37P} VLP is much smaller than that of the wild-type particle, and the CP^{S37P} VLP encapsulates shorter genetic material than the CP^{WT} VLP when expressed recombinantly (Figure S5). Since the CP^{S37P} VLP is too small to permit encapsulation of the full viral genome, we hypothesize that this mutation was not observed previously because it cannot support infection[30] of *E. coli*.

The $T = 1$ geometry is favored in the case of CP^{S37P} despite surprisingly strong similarities between the CP^{WT} and CP^{S37P} dimer structures. Investigation into the assembled structure revealed that key structural changes occur at the dimer−dimer interface. The interdimer angle between neighboring dimers was smaller in the CP^{S37P} VLP than in the CP^{WT} VLP, as expected given the formation of a smaller $T = 1$ icosahedral supramolecular assembly. We speculated that this change in interdimer interaction was due to differences in hydrogen bonding. Indeed, several side chains near residue 37 are positioned differently in the CP^{S37P} structure as compared to the CP^{WT} structure, resulting in different sets of hydrogen-bonding interactions at the dimer−dimer interface. In particular, the *cis* configuration of Pro37 appears to change the conformation of the side chain of Asn36 to interact with Asn98, favoring a reconfiguration of the hydrogen-bonding interactions and changing the positioning and angle of the dimer−dimer contact. Two hydrogen bonds were identified in the CP^{S37P} VLP near the Pro37 residue: the first between the carbonyl oxygen of Ile94 and the backbone nitrogen of Ser39 and the second between the side-chain oxygen of Asn98 and the nitrogen of the Asn36 side chain (Figure 2). In the wild-type structure, on the other hand, a hydrogen bond forms between the backbone nitrogen of Asn98 and the side-chain oxygen of Asn36.

To investigate the importance of these interdimer interactions in the CP^{S37P} VLP, we mutated the engineered *cp* gene to disrupt the potential hydrogen bonds described above, substituting an alanine at the Asn36 and Asn98 residues to create the double mutants $CP^{S37P/N36A}$ and $CP^{S37P/N98A}$ and the triple mutant $CP^{S37P/N36A/N98A}$. The resulting variants formed a mixed population of VLPs, comprising both 27 and 17 nm particles, as judged by TEM (Figure 2 and Figure S5). Surprisingly, both the $T = 3$ and $T = 1$ icosahedral conformations are apparently accessible to the CP^{S37P} mutant when either or both of these hydrogen bonds are disrupted. However, the stability of these particles, as indicated by their melting temperature, was less than that of both CP^{WT} and CP^{S37P} VLPs (Table S2). We conclude that the hydrogen-bond interaction between residues 36 and 98 stabilizes the $T = 1$ configuration of CP^{S37P} VLPs to a larger degree than the $T = 3$ configuration of CP^{S37P} VLPs. We also generated the analogous single-point mutations in the wild-type *cp* gene, yielding CP^{N36A} and CP^{N98A} proteins. The corresponding VLPs formed wild-type size particles of 27 nm diameter, as determined by TEM (Figure 2 and Figure S6), but also had lower melting temperatures (Table S2). The assembly of these proteins into VLPs of wild-type size indicates that the other interdimer interactions that remain are sufficient to result in the formation of wild-type-like VLPs. Moreover, it suggests that energetic considerations beyond hydrogen bonding may be relevant to VLP formation.

We next turned our attention to evaluating the utility of this particle in established *in vitro* techniques designed for CP^{WT} VLPs. The CP^{WT} VLP can be reassembled *in vitro* to

DOI: 10.1021/acs.nanolett.6b02948
Nano Lett. 2016, 16, 5944−5950

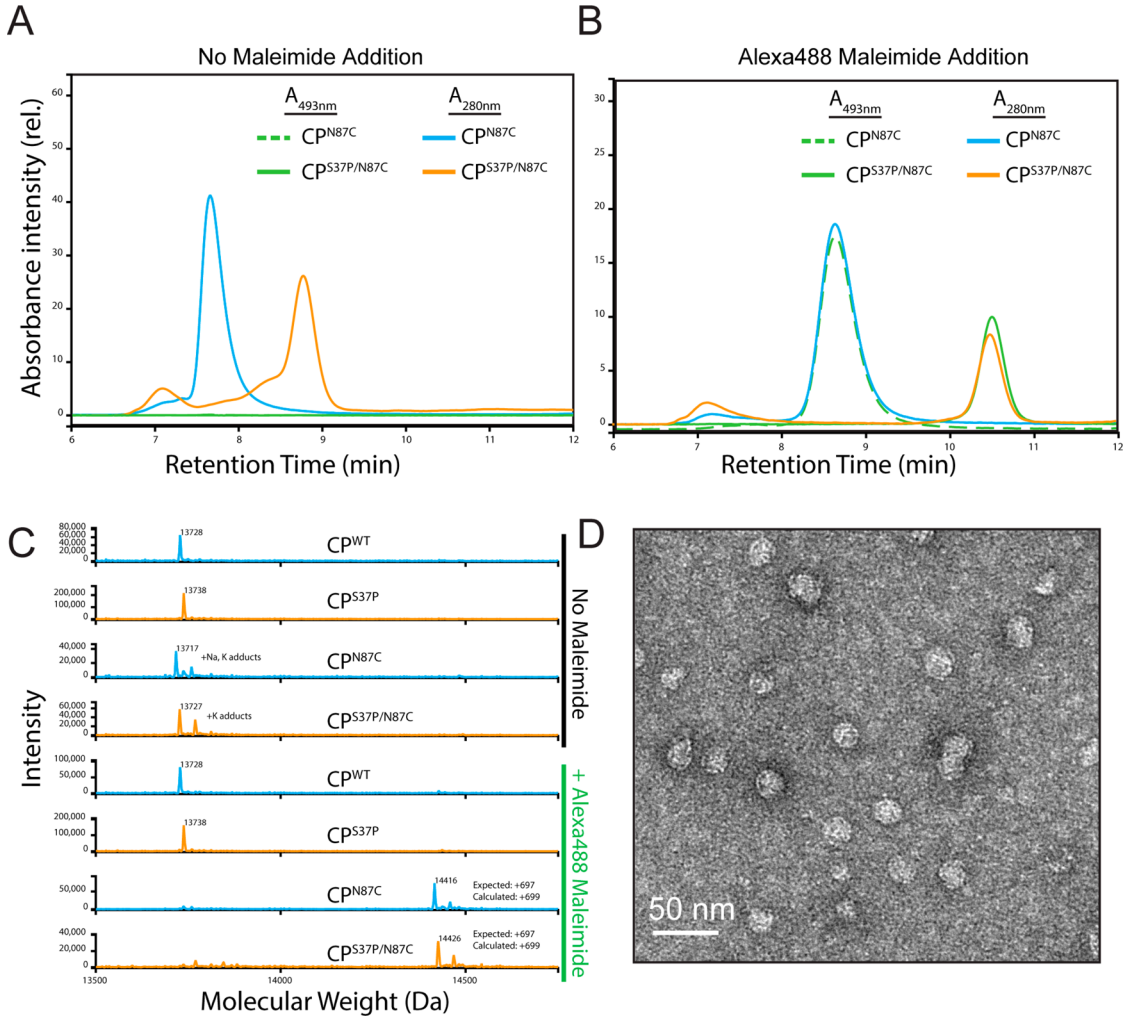

Figure 3. $CP^{S37P/N87C}$ VLPs are amenable to specific chemical conjugation with Alexa488 maleimide. Absorbance at 493 nm (A_{493}; green traces) and at 280 nm (A_{280}; blue/orange traces) of effluent from size exclusion chromatography of VLPs formed of CP^{N87C} (green dashed and blue traces) or $CP^{S37P/N87C}$ (green solid and orange traces) without (A) or with (B) maleimide addition. (C) Mass spectrometry of SEC effluent of VLPs formed of CP^{WT} CP^{N87C} (blue traces) or CP^{S37P}/$CP^{S37P/N87C}$ (orange traces) or and without maleimide addition. (D) Transmission electron micrograph of VLPs formed of $CP^{S37P/N87C}$.

encapsulate RNA, DNA, negatively charged polymers, or proteins bearing a negatively charged peptide tag. As such, it is a useful biotechnological system for applications such as the delivery of a nucleic acid, protein, or small-molecule payload to cells by receptor-mediated endocytosis[31,1,32] as well as applications in nanoscale patterning and studies of enzyme encapsulation. Indeed, we find that VLPs composed of CP^{S37P} possess many of the same useful properties as VLPs formed of wild-type CP. For example, CP^{N87C} is a useful variant that provides a cysteine residue in the VLP interior for modification via maleimide conjugation chemistry.[20] We found that $CP^{S37P/N87C}$ formed VLPs of 17 nm diameter amenable to small molecule conjugation using Alexa Flour 488 maleimide, similarly to wild-type CP VLPs (Figure 3). Moreover, VLPs comprising the CP^{S37P} variant could be disassembled and reassembled around negatively charged cargo *in vitro* in similar conditions to those identified for wild-type MS2 (Figure 4).[14] Interestingly, when disassembled dimers from both CP^{WT} and CP^{S37P} were combined at varying molar ratios, the resulting population of VLPs comprised both 17 and 27 nm sized VLPs, as determined by size exclusion chromatography and TEM. LC-MS analysis of SEC fractions indicated that the smaller population primarily consisted of CP^{S37P} protein and the larger population of CP^{WT}, suggesting that the two variants predominantly assemble separately.

We next evaluated whether the CP^{S37P} mutation behaves similarly to wild-type MS2 phage particle during the first stage of its infectious life cycle. Given the high mutation rate of single-stranded RNA viruses, we expect that this single base pair mutation occurs frequently in nature and that the resulting particles might be capable of interacting with the *E. coli* host. We therefore examined the ability of CP^{S37P} VLPs to incorporate the MS2 Mat protein, also known as the Assembly (A) protein. The Mat protein is required for infection of F^+ *E. coli* and is thought to interact with wild-type capsid C/C dimer at the 2-fold axis.[33] When the genes encoding both CP^{WT} and Mat are expressed simultaneously, approximately one Mat protein is incorporated into each CP^{WT} VLP.[19] When we isolated CP^{S37P} VLPs produced in this manner and analyzed their protein content by gel electrophoresis, a band was evident at the expected molecular weight of the Mat protein, and its identity was confirmed as the Mat protein by mass spectrometry (Table S3). Since the smaller particles are too small to encapsulate an infectious MS2 genome, we applied

DOI: 10.1021/acs.nanolett.6b02948
Nano Lett. 2016, 16, 5944−5950

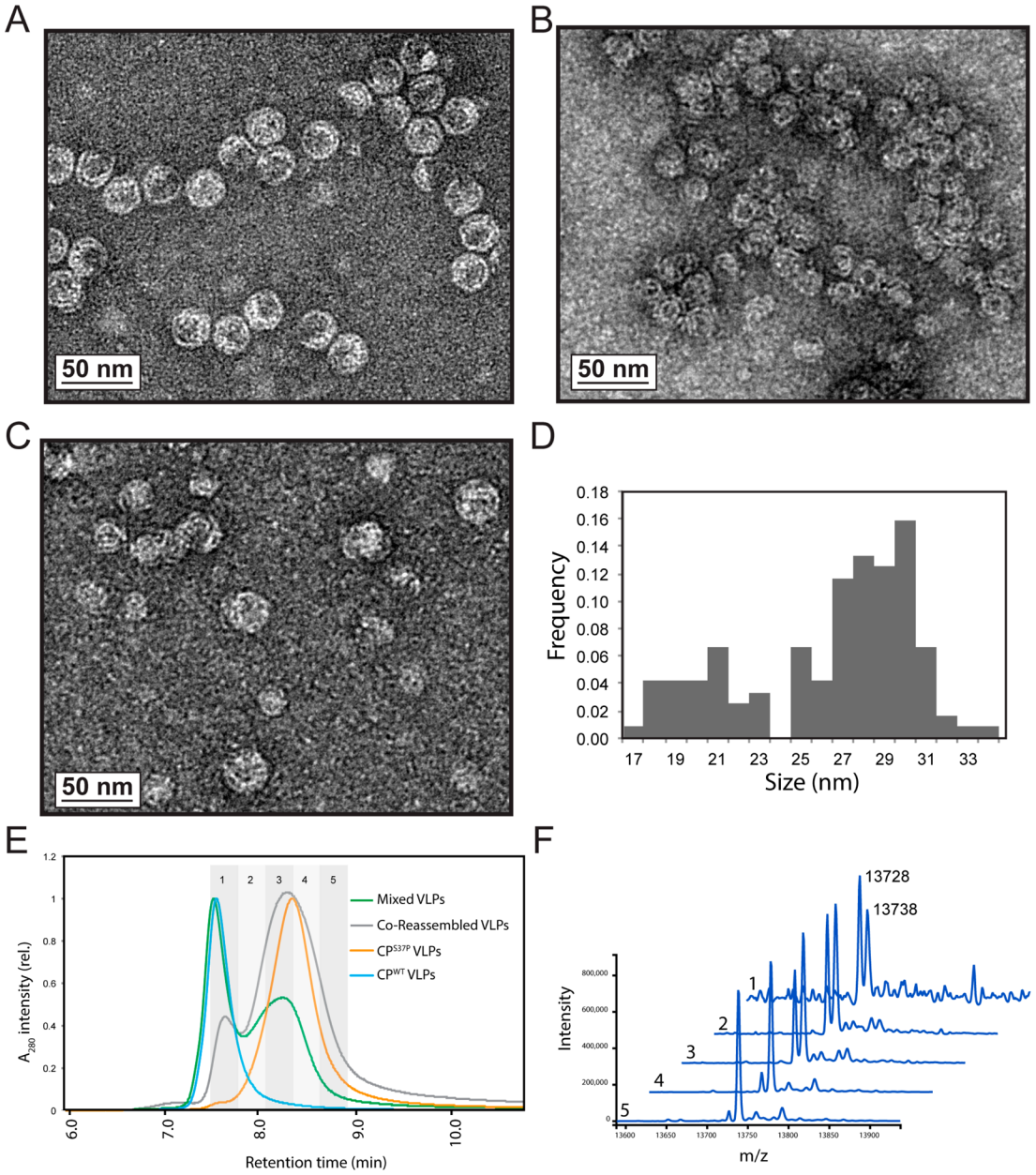

Figure 4. CP^{S37P} dimers reassemble *in vitro* to form VLPs. Transmission electron micrographs of VLPs reassembled *in vitro* from dimers of (A) CP^{WT}, (B) CP^{S37P}, and (C) a 4:1 molar mixture of CP^{WT} and CP^{S37P} dimers. (D) Histogram of VLP size determined from transmission electron micrograph of VLPs reassembled *in vitro* from a 1:1 molar mixture of CP^{WT} and CP^{S37P} dimers. (E) Absorbance at 280 nm (A_{280}) of effluent from size exclusion chromatography of mixed, separately assembled VLPs (green), VLPs reassembled from mixed CP^{WT} and CP^{S37P} dimers (gray), reassembled CP^{S37P} VLPs (orange), and CP^{WT} VLPs (blue). (F) Mass spectrometry of SEC effluent fractions 1−5 from VLPs reassembled from mixed CP^{WT} and CP^{S37P} dimers as indicated in the gray A_{280} trace in (E). CP^{WT} m/z is approximately 13 728; CP^{S37P} m/z is approximately 13 738.

these VLPs to a culture of MS2-susceptible F^+ *E. coli* and observed attachment of CP^{S37P} VLPs to the F-pilus, in lieu of a plaque assay to identify infectious virions. We found that CP^{S37P} VLPs attached in a manner similar to that observed for the CP^{WT} VLP, as assessed by examination of the pili by TEM (Figure 5 and Figure S7). This indicates that the CP^{S37P} mutant retains the ability to incorporate the maturation protein in the virion and thus also the ability to interact with the *E. coli* surface like an infectious particle.

The observation that a single amino acid change to the MS2 CP protein can mediate a stable switch in VLP structure from a $T = 3$ to a $T = 1$ icosahedron has broad implications for engineering VLP-based nanomaterials. While previous studies demonstrated that altering assembly conditions and VLP cargo can cause perturbations in the final structure of a VLP,[34−37] the CP^{S37P} mutant described here stably and uniformly adopts the alternate $T = 1$ icosahedral structure in conditions identical to those in which the native CP adopts a $T = 3$ icosahedral structure. The close similarities in primary sequence and dimer conformation of wild-type and CP^{S37P} particles mean that the two VLPs have nearly identical chemical properties, allowing for well-controlled comparisons to be made between protein containers of different sizes (27 and 17 nm, respectively) in engineering applications. The size of the encapsulating particle is known to influence the performance of drug delivery vehicles,[17] and the size of the protein container may be similarly

DOI: 10.1021/acs.nanolett.6b02948
Nano Lett. 2016, 16, 5944−5950

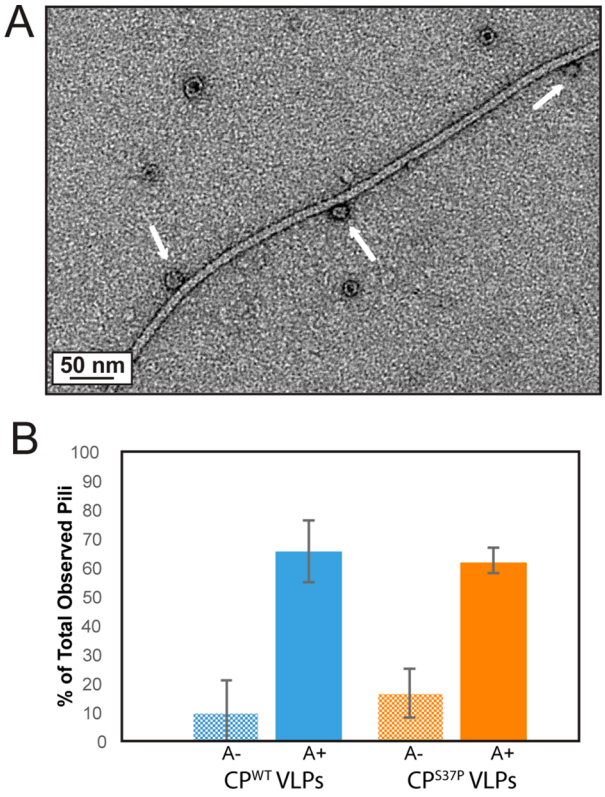

Figure 5. CP^{S37P} VLPs incorporate the Mat protein and attach to the F pilus of *E. coli*. (A) Transmission electron micrographs of CP^{S37P} VLPs aligned to *E. coli* F pilus (as indicated by white arrows). (B) Histograms of fraction of CP^{WT} (blue) and CP^{S37P} (orange) VLPs aligned to *E. coli* F pilus with (A+) and without (A−) coexpression of the Mat protein.

important in the design of nanobioreactors to immobilize and guide enzymatic pathways.

We expect our selection strategy, in which a diversified library of coat protein gene mutants was subjected to a chromatographic selection for assembly, to extend to other virus-like particle systems. In principle, any virus-like particle that encapsulates its corresponding genetic material could be subjected to a selection for assembly (whether by chromatography or otherwise), and assembly competent variants could likewise be identified by deep sequencing of the selected pool. Future investigations of the MS2 VLP may also reveal other possible geometries, perhaps including the much larger $T = 7$ icosahedral geometry. Furthermore, future selections could incorporate other selective pressures.

A deeper understanding of the sequence−structure relationship is critical if we wish to fully realize the potential of nanoscale, protein-based assemblies. Our work offers an excellent case study for researchers trying to identify the key features important to multiprotein structure formation. It is apparent that subtle changes in protein structure, and in particular in intermolecular interactions, can manifest as significant changes in the higher-order structure adopted by a multiprotein complex. Efforts to computationally predict the structure of multiprotein complexes and to design multiprotein structures *de novo* are still underway, and the behavior we observed in the case of the MS2 coat protein will be a valuable test case for methods to predict the structures of multiprotein assemblies. The change in interdimer angle seen in the CP^{S37P} $T = 1$ icosahedral assembly as compared to the wild-type VLP occurs despite very little evident change in the conformation of the dimers themselves. While hydrogen bonding seems to contribute to the stability of the smaller $T = 1$ icosahedral structure, other factors also contribute to the accessibility of the $T = 1$ icosahedral structure to the CP^{S37P} mutant. Together, our experiments suggest that fine-grained models of protein−protein interactions will be required to fully describe the effects responsible for the $T = 3$ to $T = 1$ icosahedral transition we observed. Simulating these interactions for large structures made up of many protein subunits, such as viral capsids, is a uniquely challenging problem, but with exciting possibilities if successful. In particular, resulting advances in the prediction algorithms could be applied to the design and engineering of new VLP structures as well as to the study of virus evolution.

■ ASSOCIATED CONTENT

Supporting Information

The Supporting Information is available free of charge on the ACS Publications website at DOI: 10.1021/acs.nanolett.6b02948.

Amino acid abundance of the selected library, additional characterization of VLPs, nucleic acids and Mat protein, electron micrographs of F pilus attachment, crystallographic data, and detailed materials and methods (PDF)

■ AUTHOR INFORMATION

Corresponding Author

*E-mail ercek@northwestern.edu (D.T.-E.).

Author Contributions

M.A.A. and N.M.M. contributed equally. M.A.A., N.M.M., C.M.J., E.C.H., J.E.G., and D.T.E. conceived the project, analyzed data, and designed the experiments; M.A.A., N.M.M., and E.C.H. carried out the experiments; M.A.A., B.S., and P.H.Z. collected diffraction data and solved the crystal structure; all authors wrote the paper and approved the final text.

Notes

The authors declare no competing financial interest.

■ ACKNOWLEDGMENTS

The authors thank members of the Francis and Tullman-Ercek laboratories for their assistance and for fruitful discussions, especially Dr. Adel Elsohly and Ioana Aanei. We thank the following collaborators: those at UC Davis Campus Mass Spectrometry Facilities including Dr. William Jewell and Dr. Armann Andaya; Kevin Doxzen and the Doudna lab for crystallization assistance; and the QB3 Vincent J. Coates Genomics Sequencing Laboratory, UC Berkeley. This work was supported by the National Science Foundation (award MCB1150567 to D.T.E.), the Army Research Office (grant W911NF-15-1-0144 to D.T.E.), a Knowledge Build grant from ExxonMobil Corporation (to D.T.E.), the Hellman Family Faculty Fund (to D.T.E.; J.E.G.), a UC Berkeley Fellowship (C.M.J.), a NDSEG Graduate Fellowship (E.C.H.), and a NIH T32 CBI Training Grant (grant GM066698; E.C.H.). The Berkeley Center for Structural Biology is supported in part by the National Institutes of Health, National Institute of General Medical Sciences, and the Howard Hughes Medical Institute. The Advanced Light Source is supported by the Director, Office of Science, Office of Basic Energy Sciences, of the U.S. Department of Energy under Contract DE-AC02-05CH11231.

DOI: 10.1021/acs.nanolett.6b02948
Nano Lett. 2016, 16, 5944−5950

REFERENCES

(1) Galaway, F. A.; Stockley, P. G. *Mol. Pharmaceutics* **2013**, *10* (1), 59−68.
(2) Anderson, E. A.; Isaacman, S.; Peabody, D. S.; Wang, E. Y.; Canary, J. W.; Kirshenbaum, K. *Nano Lett.* **2006**, *6* (6), 1160−1164.
(3) Obermeyer, A. C.; Capehart, S. L.; Jarman, J. B.; Francis, M. B. *PLoS One* **2014**, *9* (6), e100678.
(4) Mateo, C.; Palomo, J. M.; Fernandez-Lorente, G.; Guisan, J. M.; Fernandez-Lafuente, R. *Enzyme Microb. Technol.* **2007**, *40* (6), 1451−1463.
(5) Comellas-Aragonès, M.; Engelkamp, H.; Claessen, V. I.; Sommerdijk, N. A. J. M.; Rowan, A. E.; Christianen, P. C. M.; Maan, J. C.; Verduin, B. J. M.; Cornelissen, J. J. L. M.; Nolte, R. J. M. *Nat. Nanotechnol.* **2007**, *2* (10), 635−639.
(6) de la Escosura, A.; Nolte, R. J. M.; Cornelissen, J. J. L. M. *J. Mater. Chem.* **2009**, *19* (16), 2274.
(7) Miller, R. A.; Stephanopoulos, N.; McFarland, J. M.; Rosko, A. S.; Geissler, P. L.; Francis, M. B. *J. Am. Chem. Soc.* **2010**, *132* (17), 6068−6074.
(8) Douglas, T.; Young, M. *Nature* **1998**, *393* (6681), 152−155.
(9) Knez, M.; Bittner, A. M.; Boes, F.; Wege, C.; Jeske, H.; Mai*β*, E.; Kern, K. *Nano Lett.* **2003**, *3* (8), 1079−1082.
(10) Hooker, J. M.; Kovacs, E. W.; Francis, M. B. *J. Am. Chem. Soc.* **2004**, *126* (12), 3718−3719.
(11) Kovacs, E. W.; Hooker, J. M.; Romanini, D. W.; Holder, P. G.; Berry, K. E.; Francis, M. B. *Bioconjugate Chem.* **2007**, *18* (4), 1140−1147.
(12) Capehart, S. L.; Coyle, M. P.; Glasgow, J. E.; Francis, M. B. *J. Am. Chem. Soc.* **2013**, *135* (8), 3011−3016.
(13) O'Neil, A.; Reichhardt, C.; Johnson, B.; Prevelige, P. E.; Douglas, T. *Angew. Chem., Int. Ed.* **2011**, *50* (32), 7425−7428.
(14) Glasgow, J. E.; Capehart, S. L.; Francis, M. B.; Tullman-Ercek, D. *ACS Nano* **2012**, *6* (10), 8658−8664.
(15) Dergunov, S. A.; Durbin, J.; Pattanaik, S.; Pinkhassik, E. *J. Am. Chem. Soc.* **2014**, *136* (6), 2212−2215.
(16) Patterson, D. P.; Schwarz, B.; Waters, R. S.; Gedeon, T.; Douglas, T. *ACS Chem. Biol.* **2014**, *9* (2), 359−365.
(17) Waite, C. L.; Roth, C. M. *Crit. Rev. Biomed. Eng.* **2012**, *40* (1), 21−41.
(18) Stockley, P. G.; Stonehouse, N. J.; Valegård, K. *Int. J. Biochem.* **1994**, *26* (10), 1249−1260.
(19) Geraets, J. A.; Dykeman, E. C.; Stockley, P. G.; Ranson, N. A.; Twarock, R. *PLoS Comput. Biol.* **2015**, *11* (3), e1004146.
(20) Wu, W.; Hsiao, S. C.; Carrico, Z. M.; Francis, M. B. *Angew. Chem., Int. Ed.* **2009**, *48* (50), 9493−9497.
(21) Stonehouse, N. J.; Stockley, P. G. *FEBS Lett.* **1993**, *334* (3), 355−359.
(22) Carrico, Z. M.; Romanini, D. W.; Mehl, R. A.; Francis, M. B. *Chem. Commun.* **2008**, No. 10, 1205−1207.
(23) Valegård, K.; Liljas, L.; Fridborg, K.; Unge, T. *Nature* **1990**, *345* (6270), 36−41.
(24) Golmohammadi, R.; Valegård, K.; Fridborg, K.; Liljas, L. *J. Mol. Biol.* **1993**, *234* (3), 620−639.
(25) Stonehouse, N. J.; Valegård, K.; Golmohammadi, R.; van den Worm, S.; Walton, C.; Stockley, P. G.; Liljas, L. *J. Mol. Biol.* **1996**, *256* (2), 330−339.
(26) Axblom, C.; Tars, K.; Fridborg, K.; Orna, L.; Bundule, M.; Liljas, L. *Virology* **1998**, *249* (1), 80−88.
(27) Chackerian, B.; Caldeira, J. do C.; Peabody, J.; Peabody, D. S. *J. Mol. Biol.* **2011**, *409* (2), 225−237.
(28) Peabody, D. S. *EMBO J.* **1993**, *12* (2), 595−600.
(29) Peabody, D. S.; Al-Bitar, L. *Nucleic Acids Res.* **2001**, *29* (22), e113.
(30) Fiers, W.; Contreras, R.; Duerinck, F.; Haegeman, G.; Iserentant, D.; Merregaert, J.; Min Jou, W.; Molemans, F.; Raeymaekers, A.; Van den Berghe, A.; Volckaert, G.; Ysebaert, M. *Nature* **1976**, *260* (5551), 500−507.
(31) Ashley, C. E.; Carnes, E. C.; Phillips, G. K.; Durfee, P. N.; Buley, M. D.; Lino, C. A.; Padilla, D. P.; Phillips, B.; Carter, M. B.; Willman, C. L.; Brinker, C. J.; Caldeira, J. do C.; Chackerian, B.; Wharton, W.; Peabody, D. S. *ACS Nano* **2011**, *5* (7), 5729−5745.
(32) Glasgow, J.; Tullman-Ercek, D. *Appl. Microbiol. Biotechnol.* **2014**, *98* (13), 5847−5858.
(33) Toropova, K.; Stockley, P. G.; Ranson, N. A. *J. Mol. Biol.* **2011**, *408* (3), 408−419.
(34) Fiedler, J. D.; Higginson, C.; Hovlid, M. L.; Kislukhin, A. A.; Castillejos, A.; Manzenrieder, F.; Campbell, M. G.; Voss, N. R.; Potter, C. S.; Carragher, B.; Finn, M. G. *Biomacromolecules* **2012**, *13* (8), 2339−2348.
(35) Cadena-Nava, R. D.; Comas-Garcia, M.; Garmann, R. F.; Rao, A. L. N.; Knobler, C. M.; Gelbart, W. M. *J. Virol.* **2012**, *86* (6), 3318−3326.
(36) Kler, S.; Wang, J. C.-Y.; Dhason, M.; Oppenheim, A.; Zlotnick, A. *ACS Chem. Biol.* **2013**, *8* (12), 2753−2761.
(37) Brown, A. D.; Naves, L.; Wang, X.; Ghodssi, R.; Culver, J. N. *Biomacromolecules* **2013**, *14* (9), 3123−3129.

DOI: 10.1021/acs.nanolett.6b02948
Nano Lett. 2016, 16, 5944−5950